Development of electrochromic smart windows by sol-gel techniques

B. Munro, S. Krämer, P. Zapp, H. Krug and H. Schmidt

Institut für Neue Materialien, Im Stadtwald, D-66123 Saarbrücken, Germany

ABSTRACT

A novel nanocomposite lithium ion-conducting electrolyte has been developed, based on organically modified silanes, which is suitable for application in a sol-gel electrochromic system. The system developed consists of FTO-coated (**F**luorine doped **T**in **O**xide) glass coated with tungsten oxide ,WO_3, at one side of the device as the electrochromic layer, with a cerium oxide-titanium oxide layer, CeO_2-TiO_2, acting as ion-storage layer or counter electrode. The adhesive properties of the electrolyte enabled the manufacture of electrochromic devices in a laminated structure: glass\FTO\$WO_3$\nanocomp.elect.\$CeO_2$-$TiO_2$\FTO\glass. The conductivity of the nanocomposite electrolyte system varies between 10^{-4} and 10^{-5} Scm^{-1} at 25°C depending on the exact composition. The temperature dependence of the conductivity exhibits typical Vogel-Tamman-Fulcher (VTF) behaviour. The thickness of the electrolyte between the two halves of the device could be adjusted by the use of a spacer technique in the range 10 - 150 μm. Optoelectrochemical measurements were conducted on electrochromic devices to study the kinetics of colouration and bleaching as a function of the number of switching cycles. At present, cells are constructed in two formats: 10 x 15 cm^2 and 35 x 35 cm^2. Switching times under one minute were achieved for the smaller format with a corresponding optical modulation between 75% to 20% (at λ = 0.633 μm). In the case of the larger format the switching time increases to several minutes due to the increase in geometric area.

Keywords: nanocomposite electrolyte, electrochromism, smart windows, sol-gel, tungsten oxide

1. INTRODUCTION

In recent years, there has been a vast amount of research and development conducted at both university[1-4] and company level[5-11] into electrochromism, due to the variety of potential applications, which exist for electrochromic devices, ie. antiglare rearview mirrors[7,8], sun-rooves[9] and for smart windows[8]. However, at present only small-area devices such as the antiglare-mirrors from the Donnelly Corporation or from GENTEX are commercially available. The reasons why larger area devices are not yet available are manifold. One main reason is the physical deposition techniques normally employed to coat glass substrates with the electrochromic layers and ion-storage layers. Sputtering, although it supplies coatings of a very high quality involves high capital investment costs. Therefore, the mian objective of our work has been to develop an all sol-gel electrochromic system for large-area applications with its inherent advantages of low cost thin films by conventional wet-chemical coating techniques and chemical flexibility.

The material of choice for the electrochromic layer is of course tungsten oxide, WO_3. due to its high colouration efficiency depending on wavelength of between 40 cm^2/C (550 nm)[5] and 130 cm^2/C (800 nm)[5] and several different sol-gel routes have been developed based on different starting compounds have been reported[12]. Sols based on the hydrolysis and condensation of tungsten alkoxides[13] may be employed to form WO_3-layers, however the cost of the precursors is limits the potential of this route for a commercial application. Layers prepared from tungsten oxychloride, $WOCl_4$, have been reported[14] as having very good properties in laboratory investigations. Sols have to be handled in a dry inert atmosphere and there may be problems with the long-term electrochemical stability of such layers due to residual chloride. Synthesis of WO_3-layers by a peroxotungstic acid[10,11] has several advantages in that the starting materials, namely tungsten metal powder and hydrogen peroxide solution, are relatively inexpensive and that WO_3 layers can be obtained at low firing tempertaures. Therefore, in this work a modified peroxotungstic acid route was developed under consideration of criteria such as sol stability and the potential for scaling-up, which are relevant for large area applications.

The counter electrode or ion-storage layer should either colour in a complementary manner ie. anodically, whilst the electrochromic layer colours cathodically or should permit ion insertion and deinsertion without a significant change in transmission. The cerium oxide-titanium oxide system was chosen as a colourless passive ion-storage layer as first proposed by Aegerter and Baudry[15]. Vanadium pentoxide[16] has also been considered as a potential ion-storage layer due to its good intercalation properties. Vanadium pentoxide colours cathodically as well as anodically so that devices constructed with V_2O_5 have no true colourless state.

Another problem is that tungsten oxide layers and therefore also complete cells exhibit a swinging-in behaviour[11]. The colouration of the layers is low at the beginning of cycling but increases with the number of cycles. Furthermore, this effect has been found[17] to be associated with the irreversible intercalation of a fraction of the lithium ions, which do not lead to colouration. Ways to counteract this effect are therefore based on pre-loading the tungsten oxide layer with lithium, by electrochemically charging the layers with lithium ions from a liquid electrolyte before mounting the cells with polymer electrolyte or by dry lithiation[18].

One of the key elements is the ion-conductive transparent electrolyte. There are several problems connected with the type of electrolyte, which may be employed. Small area devices can be constructed, which either contain a liquid or semi liquid electrolyte[1], best known example being $LiClO_4$ dissolved in propylene carbonate (PC), sufficient reliability with respect to the sealing of the units being a prerequisite, so that there is no problem in relation to safety. Thin films of hydrated oxides have also been employed for this purpose, for example tantalum oxide, Ta_2O_5 [19]. Although the latter functions excellently in small area devices the coating of large areas with such thin films without defects is problematic. Indeed, thin film ceramic lithium conductors have been prepared e.g. $LiNbO_3$, however the conductivity is not particularly high and so thin films are again required[18].

Polymer electrolytes[20] or polymer gel electrolyte systems offer a reasonable alternative with ionic conductivties of up to 10^{-3} Scm^{-1} but tend to exhibit an insuffucient long-term UV-stability and poor form stability. Examples of polymer electroytes include those based on $LiClO_4$ or a another lithium salt dissolved in polyethylene oxide, PEO, polypropylene oxide, PPO, polyethylene imide, PEI[21] . Such polymers tend to have a rather low conductivity at room temperature 10^{-6} - 10^{-7} S/cm. Proton conducting polyAMPS systems[2,20] (poly(2-acrylamido-2-methyl-2-methylpropanesulphonic acid) first have to be be conditioned in 65-70% humidity to acheive high conductivities and are therefore expected to suffer from long-term stability problems.

A solid Li^+ conducting nanocomposite electrolyte has been described[22], based on organically modified silanes. In this paper the role of the electrolyte in an electrochromic system is considered and the investigation of important properties necessary for electrochromic applications is described.

2. EXPERIMENTAL

2.1 Syntheses

A solid ionic conductor has been developed, based on glycidoxypropyltrimethoxysilane (GPTS), tetraethoxysilane (TEOS), $LiClO_4$,, $Zr(O^nPr)_4$ and tetraethylene glycol (TEG). GPTS and TEOS serve as network formers, whereas TEG acts as a plasticizer. Lithium perchlorate is the conducting salt and $Zr(O^nPr)_4$ is added as a starter for thermal curing. Dried $LiClO_4$ is dissolved in a mixture of TEG and prehydrolysed GPTS. TEOS and $Zr(O^nPr)_4$ are then added. Volatiles are removed by rotary evaporation immediately prior to application to the coated ITO-substrates. The cell containing electrolyte is heat treated at 100°C for several hours to allow thermal curing to occur. The thickness of the electrolyte layer is set between 12 and 15 μm after curing.

The remaining synthesis routes have already been described in detail elsewhere[22] and so will only be briefly described here. Stable tungsten oxide coating sols were synthesized using a route based on the dissolution of tungsten metal powder in an excess of hydrogen peroxide solution (30%), in the presence of ethanol and glacial acetic acid, to give peroxotungstic acid.

The CeO_2-TiO_2-Sol[22] was synthesized using cerium (III) nitrate hexahydrate, $Ce(NO_3)_3.6H_2O$, and titanium isopropylate, $Ti(O^iPr)_4$, as precursors, in an equimolar ratio.

Glass substrates with an ITO layer (Donnelly Applied Films, 12 Ω/) or an FTO layer (Libbey-Owens-Ford, 10 Ω/) were coated by dip coating under contolled conditions of relative humidity and temperature. Tungsten oxide layers 250 nm thick and CeO_2-TiO_2 layers 140 nm could be obtained in a single coating step[22]. Substrates up to 35 x 35 cm^2 in size have been coated in this way.

2.2 Conductivity Measurements

The ionic conductivity was determined by impedance spectroscopy employing a Zahner IM5d electrochemical impedance analyser. The frequency range was 1 Hz - 1 MHz and the amplitude of the applied a.c.potential was 50 mV. Electrolyte samples were thermally cured on interdigited capacitor, IDC, structures (Au on Al_2O_3). IDC´s were chosen for the measurement because they represent a reliable reproducible electrode geometry. Samples were first heated under vacuum in a specially constructed measurement cell to remove absorbed water and impedance measurements were first conducted on cooling. The conductivity values were thus determined in the range 293 - 383 K. In addition, d.c polarisation experiments were conducted on samples employing an EG & G PARC 273A Potentiostat in order to estimate the ionic transport number. A very low electronic contribution to the total conductivity is necessary to ensure a good memory effect in electrochromic devices.

2.3 Spectroscopic determination of electrolyte thickness

UV-VIS spectra obtained for complete EC-cells with a multichannel UV-VIS spectrometer (ZEISS SPECORD 10) exhibit an interference pattern caused by multiple reflections of the measurement beam between the glass substrates. This effect could be exploited to determine the thickness of the electrolyte once the refractive index of the electrolyte had been measured.

2.4 Optoelectrochemical characterisation

Optoelectrochemical measurements were conducted on EC cells constructed with nanocomposite electrolyte in two formats: 10 x 15 cm^2 and 35 x 35 cm^2.

Complete cells were poled between +2.0 and -2.5 V in order to study the coloration and bleaching kinetics. On switching, the average transmission over the wavelength range 380 -800 nm was measured as a function of time, employing a multichannel UV-VIS spectrometer (ZEISS SPECORD S10). Colouring times were defined as the time between 90% of the initial transmission, T_0, and 110% of the final transmission, T_x, bleaching times were similarly defined. The change in optical density, ΔOD, was also taken as an important criterion for assessing the electrochromic layers, whereby:

$$\Delta OD_x^{(380-800nm)} = \log (T_0^{(380-800nm)} / T_x^{(380-800nm)}) \qquad (1)$$

In-house constructed potentiostats were employed to switch several cells simultaneously for large numbers of cycles. The variation in ΔOD and in the switching times were investigated as function of the number of cycles. To determine the amount of charge incorporated during cycling and the colouration efficiency then dynamic transmissions measurements were conducted parallel to chronamperometric measurements with a EG&G PARC 270 Potentiostat.

2.5 Thermal analysis

Differential scanning calorimetry measurements were conducted using with a DSC-200 (Netsch). Samples of electrolyte mixture were weighed (10 mg) into aluminium pans with a scan rate of 10 K/min in the temperature range 0 - 200°C. Aim of the measurements was to determine the optimal temperature range to carry out the curing of the electrolyte.

3. RESULTS

3.1 Electrolyte Model

One of the most important elements of the EC-system is the transparent electrolyte. In the majority of the investigations, low molecular weight polymeric systems are used, whereby the polymer has a suffucient solvating power for lithium salts. These systems however cause problems when taken for large area applications due to their low mechanical and sometimes low chemical stability. Polymersied systems with high mechanical strength show a poor diffusibility for Li^+. For this reason, a nanocompsite system has been designed which, should on the one hand allow for a high degree of diffusion and on the which, on the other hand should provide for sufficient mechanical stability[22].

For this reason, different structural elements have been employed to combine various basic properties. These are polar groups to provide to solvate Li^+, groups to build-up organic polymeric networks (epoxides), groups to build-up an inorganic backbone (Si-O-Si) and catalytically active groups for the formation of polyethylene oxide networks from epoxides and nanoparticles to give a mechanically stable nanocomposite. Based on results reported elsewhere[23, 24] for the in-situ reaction $Zr(OR)_4$ to give nanoparticles and the catalytic polymerisation from epoxysilanes by boehmite nanoparticles[24], a composite was prepared according to the following scheme (fig. 1). In addition, it is to be expected from work reported by Schmidt et al.[25], that as well as Zr-alkoxides, ZrO_2 nanoparticles also catalyse the epoxide polymerisation.

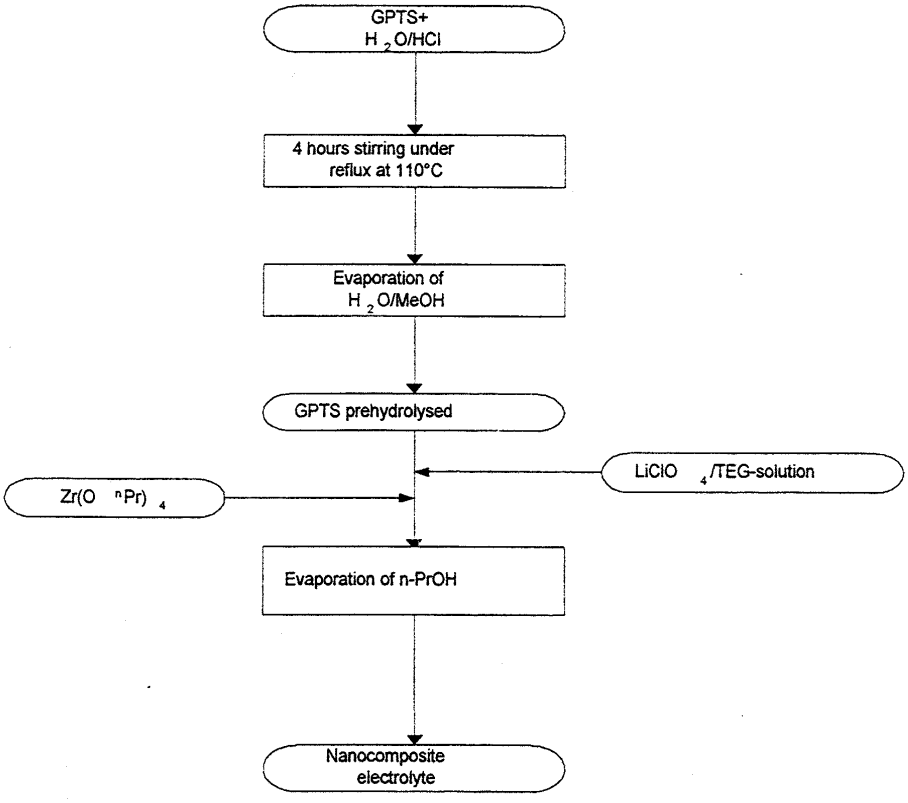

Figure 1: Flow diagram showing the synthesis principles for the nanocomposite electrolyte.

DSC measurements (figure 2.) show an exothermic peak due to the polymeristation (epoxide ring opening) which has a maximum at 115 °C and therefore the curing of the electrolyte was conducted above 100 °C. DSC measurements on heat treated samples did not exhibit this peak showing that the polymerisation was complete.

Due to the particle hydrolysis and condensation, the viscosity of the composite was adjusted in a such a way that layer thicknesses up to 15 µm were obtained. This allows the mounting of large area cells (35 x 35 cm^2, at present) without

running the risk of short circuit hazards. In figure 2, a model of the composite is given.. In high-resolution transmission electron microscopy, no nanoparticles could be detected but from investigations on similar preparations[26], one can conclude that ZrO_2-particles in the range of about 2 nm are present. A model of the composite is given in figure 3.

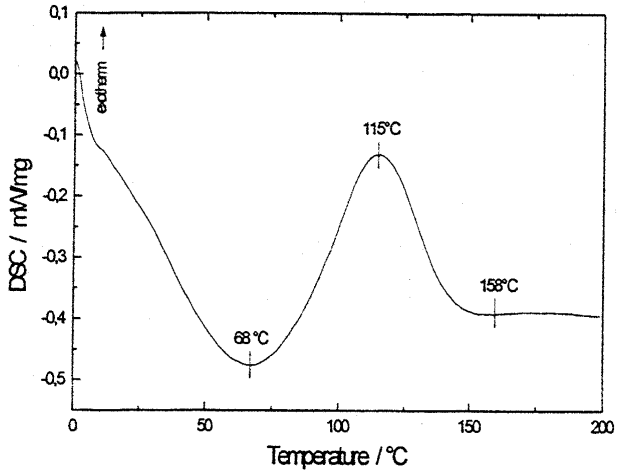

Figure 2: **DSC plot for electrolyte mixture showing a strong exotherm for the polymerisation with maximum at 115 °C.**

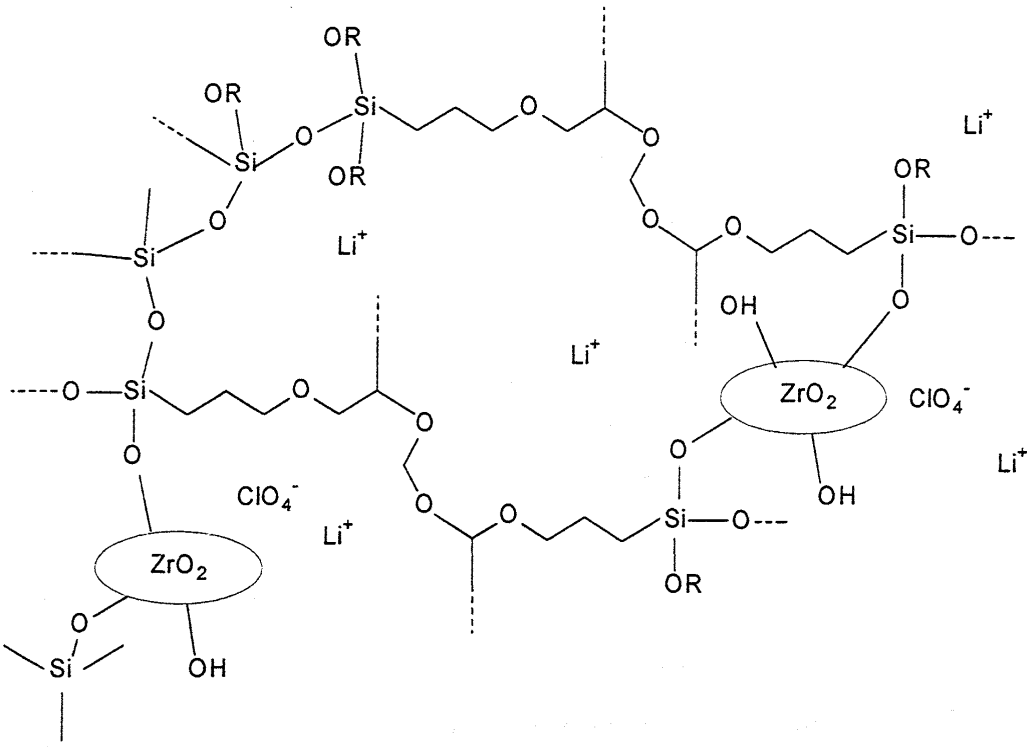

Figure 3: Model of the nanocomposite electrolyte structure

After mounting the two glass panes, the system is cured by thermal treatment at 100°C and the polyethylene oxide formation occurs via the catalytic effect of the Zr-alkoxide. At the same time, the electrolyte acts as an adhesive sealing the two panes together. The conductivity was measured by impedance spectroscopy.

3.2 Conductivity measurements

Figure 4 shows an Arrhenius plot for a nanocomposite electrolyte. The slightly curved plot is indicative of Vogel-Tammen-Fulcher behaviour, as is normally observed for polymeric electrolyte systems[21]. VTF plots are described by the following equation:

$$\sigma = \frac{A}{\sqrt{T}} * \exp\left[-\frac{E_a}{R(T - T_0)}\right] \qquad (2)$$

where s is the ionic conductivity in S/cm, T is temperature in K, To is the ideal glass transition temperature, A is the pre-exponential factor and E_a is the so-called pseudo-activation energy in kJ/mol.

The ionic conductivity for the sample shown in figure 4 is 1.64 x 10^{-5} S/cm at 298 K. D.c polarsiation measurements indicate that the contribution of electronic conductivity to the total conductivity is very small with $\sigma_{elect.} << 10^{-8}$ S/cm. Expressed in another way this means that the ionic transport number, t_{ion}, is greater than 0.999. Of course it is not possible with such as measurement to separate out the individual contributions to the conductivity from different ions, Li^+ or ClO_4^-

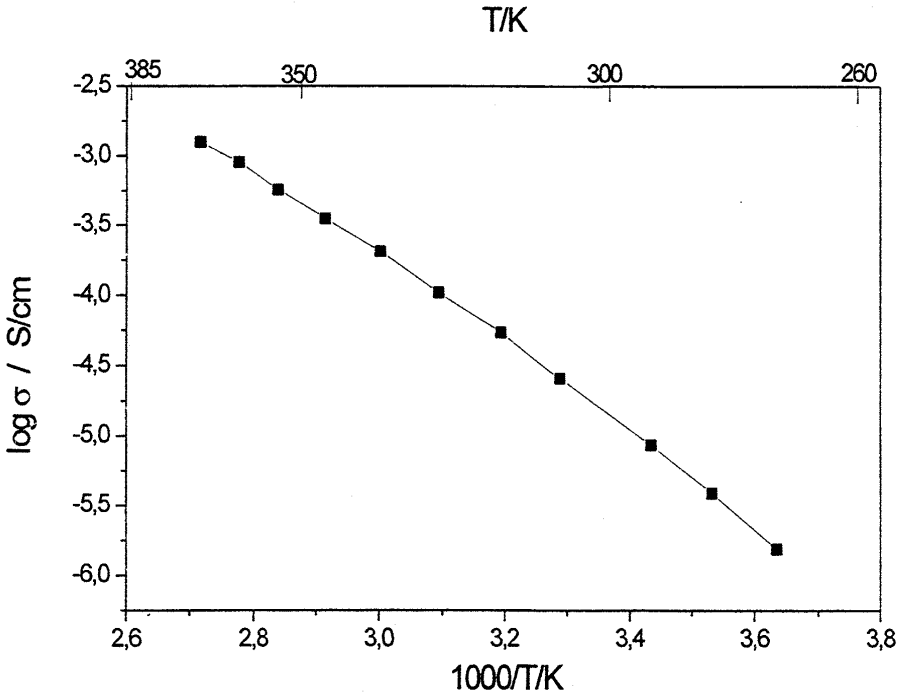

Figure 4: An Arrhenius plot of conductivity against reciprocal temperature for a nanocomposite electrolyte sample.

A conductivity model for the electrolyte consists of Li+ ion-hopping between a variety of available electronegative oxygen sites either in silanol groups, SiOH, on the surface of nanoparticles or oxygens in polyethylene oxide chains.

Figure 5 shows an UV-VIS spectrum obtained for a complete EC-cell. A waviness in the spectrum is cleary noticeable. This is caused by reflections of the beam between the glass substrates. The distance between the glass substrates, d, and hence the thickness of the electrolyte can be calculated according to the following equation:

$$d = \frac{\lambda_1 \lambda_2 (\Delta m)}{2n(\lambda_2 - \lambda_1)} \qquad (3)$$

where $\lambda 1$ and $\lambda 2$ are two wavelengths, Δm is the number of maxima between $\lambda 1$ and $\lambda 2$ and n is the refractive index. The refractive index from the electrolyte was determined separately and is approximately 1.5. For the spectrum shown the distance separating the substrates was calculated to be 12±1μm. Furthermore, the absence of short circuits between the two halves of the cells could be confirmed by electrochemical measurements. Indeed, employing this method a separation of the substrates of between 12 and 15 μm could be achieved even over areas of up to 0.1 m^2.

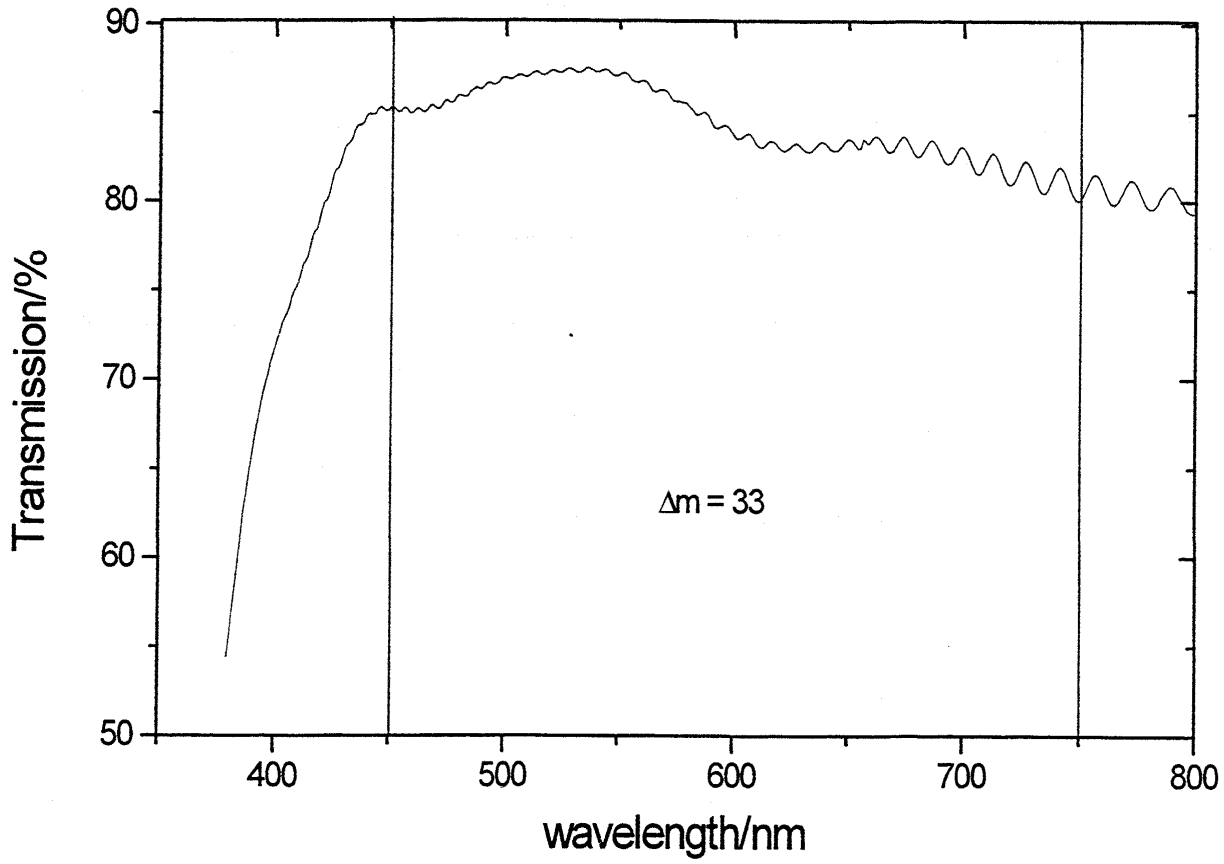

Figure 5: An UV-VIS transmission spectrum for a complete EC-cell showing waviness in the spectrum due to reflections between the glass substrates

3.3 Key data for sol-gel EC-cells

The key data for EC-cells in both formats : 10 x 15 cm^2 and 35 x 35 cm^2 are summarised in table 1. As can be seen from the table potentiostatic switching is faster than galvanostatic switching. Galvanostatic switching provides for better control of the amount charge. Furthermore, increasing the area of the device leads to an increase in switching times. This is a well-known effect and is due to the limited sheet resistance of the transparent conducting oxide layer on the glass substrates as the electrodes can only be contacted at the edges of the devices.

Table 1: Key data for sol-gel electrochromic cells in two formats: 10 x 15 cm^2 and 35 x 35 cm^2

property	cell format:10 x 15 cm^2	cell format: 35 x 35 cm^2
trans., bleached (λ = 0.633μm)	75%	75%
trans., coloured (λ = 0.633 μm)	22%	30%
potent. switching: potential range	-2.5 V (col.), +2.0 V(bl.)	-2.0 V (col.), +2.0 V (bl.)
galv. switching: current density	38 μA/cm^2	5 μA/cm^2
potent. switching time: colouring	< 100 s	< 5 min.
potent. switching time: bleaching	< 50 s	< 3 min.
galv. switching time: colouring	260 s	40 min
galv. switching time: bleaching	260 s	40 min
colouration efficiency*	45 cm^2/C	41 cm^2/s
no. of cycles:	10^5	10^5

*The galvanostatic colouration efficiency of the cells, μ, was calculated according to:

$$\mu = (\Delta OD \,.\, A)/(I \,.\, t) \qquad (4)$$

where A is the area in cm^2, I the current in ampere and t the time in s.

4. DISCUSSION

The ionic conductivity of the investigated system, namely 10^{-4}-10^{-5} Scm-1, is sufficient for large-area electrochromic applications, where switching times in the minute range are required. Polymer electrolyte systems or swollen polymer systems have been reported with much higher conductivites[20]. However, high conductivites are only achievable for systems with poor mechanical properties and the system described here also fufills a secondary adhesive function. The importance of the electronic component of the conductivity is that this must be kept as low as possible to prevent a loss in memory effect. A coloured electrochromic cell contains a separation in charge i.e it can be modelled electrically as a capacitor. Significant electronic conductivity destroys the charge separation and bleaching occurs spontaneously. Ensuring that the two sides of the device do not come into contact with one another causing internal short circuits is equal importance for the same reason.

Table 1 demonstrates the respective advantages and disadvantages of two possible methods of switching: potentiostatic or galvanostatic. With constant voltage drive the current decreases with time due to its dependence on the chemical diffusion of lithium ions in the WO_3-layer. Switching under constant current conditions the potential rises sharply at the beginning, before levelling out. The change in optical density depends on the concentration of absorbing species (Beer-Lambert Law), which is given here by the charge passed so that with potentiostatic switching rapid colouration or bleaching is achieved in the initial phase of switching. Galvanostatic switching gives a near constant rate of change of OD with time.

Potentiostatic switching is therefore suitable for small area devices where shorter switching times are required as the majority of the colouration is achieved in the first seconds of the switching process. Galvanostatic switching may be more suitable for large area applications, where the colouration may be spread over a longer time with a lower maximum potential being experienced by the cell. Galvanostatic switching also avoids the problem of the varying EMF of the cells with potentiostatic switching[27,28].

The colouration efficiency of 40-45 cm^2/C for the devices, determined as average value over the wavelength range: 380-800 nm, is a net colouration efficiency comprising the contributions from the EC-layer and the ion-storage layer. However, the colouration change associated with the CeO_2-TiO_2 layer is negligible in comparison to the WO_3-layer so that as an

approximation the value corresponds to that for the WO_3 alone. This value is comparable with literature reported systems[7], whereby most values are quoted for a definite wavelength and the colouration efficiency is known to be wavelength dependent[29].

The increase in switching times with increasing geometric area is due to the finite surface conductivity of the ITO or FTO coatings , which cause a drop in potential across the breadth of the electrodes[15].

5. CONCLUSIONS

An ion-conducting electrolyte has been developed with properties suitable for electrochromic applications. The ionic conductivity is sufficient for large area applications where the emphasis is on switching times in the minute range. In addition, the electronic contribution to the total conductivity is very low so that a long-lasting colouration can be achieved without applying a potential continually ie. there is a good memory effect. The use of a spacer technique avoids internal short circuits over large areas improving the efficiency of the devices and alos preventing loss of the memory effect.

Sol-gel nanocomposite electrolyte could be exploited to prepare electrochromic cells with very good properties. Cells of the following construction: ITO/WO_3/electrolyte/CeO_2-TiO_2/ITO were assembled in two formats: 15 x 10 cm^2 and 35 x 35 cm^2. Tests on the smaller cells gave a change in optical density of 0.6 or a change in transmission from 75% to 20% in a switching time of less than 60 s, after the initial swinging-in of the cells, when the cells were coloured potentiostatically at -2.5 V. The colouration of the cells remained homogeneous on scaling-up to the larger format, whereby potentiostatic colouration times increased to around 5 minutes for a similar degree of colouration. These devices exhibited satisfactory colouration and bleaching kinetics appropriate to large area applications for example for smart windows.

ACKNOWLEDGEMENTS

The authors would like to thank the German Ministry for Education and Research (BMBF) for their financial support of this project (3N2001A4) as part of the Matech programme. Thanks are also due to the companies Bischoff Glastechnik (BGT) and Donnelly HOHE for permitting the publication of these results.

REFERENCES

1. C. G. Granqvist, *Handbook of Inorganic Electrochromic Materials*, Elsevier, Amsterdam, 1995.
2. P. M. S. Monk, R. J. Mortimer and D. R. Rosseinsky, *Electrochromism: Fundamentals and Applications*, VCH, Weinheim, 1995.
3. C. M. Lampert, "Electrochromic Materials and Devices for Energy Efficient Windows", Sol. Energy Mater. **11**, pp. 1-28, 1984.
4. S. K. Deb, "Opportunities and Challenges of Electrochromic Phenomena", Sol. Energy Mater. **25**, pp. 327-338, (1992).
5. T. Gambke and B. Metz, "Electrochromic Layers for Active Optical Filters",Glastech. Ber. **62(2)**, pp. 38-45, (1989).
6. F. G. Baucke, K. Bange and T. Gambke, "Reflecting Electrochromic Devices", Displays **(10)**, pp. 179-189, 1988.
7. K. Bange and T. Gambke, "Electrochromic Materials for Optical Switching Devices", Adv. Mater. **2**, pp. 10-16, 1990.
8. T. Kamimori, J. Nagai and M. Mizuhashi, "Electrochromic Devices for Transmissive and Reflective Light Control", Sol. Energy Mater. **16**, pp 27-38, 1987.
9. C. G. Granqvist, "Electrochromic materials promise smart products",Opto and Laser Europe **17**, pp. 17-20, 1995.
10. M. Denesuk, J. P. Cronin, S. R. Kennedy, K. J. Law, G. F. Nielson and D. R. Uhlmann,"Coloration Behavior of Hybrid Electrochromic Films", in *Optical Materials Technology for Energy Efficiency and Solar Energy Conversion XIII*, V. Wittwer, C. G. Granqvist, C. M. Lampert, **2255**, pp.52-59, SPIE, Bellingham, 1994.
11. D. J. Taylor, J. P. Cronin, L. F. Allard Jr. and D. P. Birnie III, "Microstructure of Laser-Fired, Sol-Gel-Derived Tungsten Oxide Films", Chem. Mater. **8**, pp. 1396-1401, 1996.
12. M. A. Aegerter, "Sol-Gel Chromogenic Materials and Devices", in *Structure and Bonding*, **85**, pp 149-194, Springer, Berlin Heidelberg, 1996.

13. A. Takase and K. Miyakawa, "Raman Study on Sol-Gel Derived Tungsten Oxides from Tungsten Ethoxide", Jap. J. Appl. Phys. 30(8B), pp. L 1508 - L 1511, 1991.
14. P. Judeinstein and J. Livage, "Sol-Gel Synthesis of WO_3 Thin Films", J. Mater. Chem. **1(4)**, pp. 621-627, 1991.
15. P. Baudry, A. C. M. Rodrigues, M. A. Aegerter and L. O. Bulhoes, J. Non-Cryst. Solids **121**, pp. 319-322 , 1990.
16. J. Livage, "Vanadium Pentoxide Gels", Chem. Mater. **3**, pp. 578-593, 1991.
17. S. J. Babinec, Solar Energy Mater. **25**, pp. 269-291, 1992.
18. P. V. Ashrit, G. Bader, F. E. Giroud and V.-V. Truong, "Electrochromic Materials for Smart Window Applications", SPIE, *Optical Data Storage Technologies*, **1401**, pp. 119-129, 1990.
19. T. Kamimori, J. Nagai and M. Mizuhashi, Solar Energy Mater. **16**, pp. 27- 38 , 1987.
20. B. Scrosati, "Laminated Electrochromic Displays and Windows", in *Applications of Electroactive Polymers*, B. Scrosati, pp. 250-288, Chapmann and Hall, London, 1993.
21. M. Armand, "Polymer Solid Electroyltes - An Overview", Solid St. Ion., **9 &10**, pp. 745 - 754, 1983.
22. B. Munro, P. Conrad, S. Krämer, H Schmidt and P. Zapp, "Development of Electrochromic Cells by the Sol-Gel Process", Proc. Eurosun´96 (Freiburg, 1996) to be published in Sol.Energy. Mater.
23. P. W. Oliveira, H. Krug, H. Künstle and H. Schmidt, "The production of Fresnel lenses in sol-gel derived Ormocers by holography.", SPIE Vol. **2288** Sol-Gel Optics III, pp 554-562, 1994.
24. E. Geiter, "Herstellung und Charakterisierung von neuartigen Kratzfestbeschichtungssystemen für Kunststoffe durch Einbau von nanokristallinen Metalloxiden in eine anorganisch organische Kompositmatrix", PhD Thesis, Institut für Neue Materialien, Saarbrücken 1997.
25. H. Schmidt, B. Seiferling, G. Philip and K. Deichmann, "Development of Organic-Inorganic Hard Coatings by the Sol-Gel Process", in Ultrastructure processing of advanced ceramics: Proceedings of the Third International Conference on Ultrastructure Processing of Ceramics, Glasses and Composites, Wiley, pp. 651-660, 1988.
26. F. Tiefensee, "Untersuchung des Eigenschaftsprofils von ORMOCERen hinsichtlich ihrer Anwendung in der Integrierten Optik", PhD. Thesis, Institut für Neue Materialien, Saarbrücken 1994.
27. J. Ngai, T. Kamimori and M. Mizuhashi; Proc. Soc. Photo-Opt. Instrum. Engr. **502**, pp. 59-66, 1984.
28. J. Ngai, T. Kamimori and M. Mizuhashi; Sol. Ener. Mater. **13**, pp. 279-295, 1986.
29. S. I. Cordoba de Torresi, A. Gorenstein, R. M. Torresi and M. V. Vazquez, J. Electroanal. Chem. **318**, pp. 131-144, 1991.